Research Article Vol. 60, No. 16 / 1 June 2021 / Applied Optics 4519

applied optics

Optical design for laser tweezers Raman spectroscopy setups for increased sensitivity and flexible spatial detection

Tobias Dahlberg and Magnus Andersson*

Department of Physics, Umeå University, 901 87 Umeå, Sweden
**Corresponding author: magnus.andersson@umu.se*

Received 12 March 2021; revised 22 April 2021; accepted 28 April 2021; posted 30 April 2021 (Doc. ID 424595); published 21 May 2021

We demonstrate a method to double the collection efficiency in laser tweezers Raman spectroscopy (LTRS) by collecting both the forward-scattered and backscattered light in a single-shot multitrack measurement. Our method can collect signals at different sample volumes, granting both the pinpoint spatial selectivity of confocal Raman spectroscopy and the bulk sensitivity of non-confocal Raman spectroscopy simultaneously. Further, we display that our approach allows for reduced detector integration time and laser power. To show this, we measure the Raman spectra of both polystyrene beads and bacterial spores. For spores, we can trap them at 2.5 mW laser power and acquire a high signal-to-noise ratio power spectrum of the calcium-dipicolinic acid peaks using an integration time of 2 × 30 s. Thus, our method will enable the monitoring of biological samples sensitive to high intensities for longer times. Additionally, we demonstrate that by a simple modification, we can add polarization sensitivity and retrieve extra biochemical information.

https://doi.org/10.1364/AO.424595

1. INTRODUCTION

Laser tweezers Raman spectroscopy (LTRS) is a powerful technique that combines the manipulation capabilities of optical tweezers and the biochemical fingerprinting of Raman spectroscopy [1,2]. LTRS has been applied to study many biological systems, for example, bacteria, cells, and spores. Specifically, LTRS has been used to assess germination kinetics, spore deactivation [3,4], and red blood cell oxygenation states and interaction with silver nanoparticles [5,6]. However, spontaneous Raman scattering is a weak process, as only about 1 in 10 million excitation photons scatters in this manner. Combining this with the weak scattering inherent to many biological materials [7], we need either long integration times [8] or high excitation powers [9] to get clear Raman spectra. However, both of these solutions have adverse side effects. Long integration times cause the time resolution to suffer, making it impossible to investigate fast processes. Further, increasing the excitation power increases the rate of photodamage linearly, meaning that doubling the power halves the maximum measurements time [10].

We can avoid these problems by moving away from spontaneous Raman scattering to more sensitive Raman techniques such as coherent anti-Stokes Raman spectroscopy (CARS) or surface-enhanced Raman spectroscopy (SERS), improving sensitivity by several orders of magnitude. However, these techniques have limitations. CARS requires expensive and complicated experimental setups to realize [11], and SERS necessitates the use of expensive sample substrates that often suffer from problems with producing homogeneous and repeatable Raman signals [12]. Thus, to keep the simple experimental setup of a spontaneous Raman setup and to minimize these problems, it is desirable to make it as efficient as possible.

In this work, we show an easy way of doubling an LTRS setup's collection efficiency. We modify an LTRS setup working in the backscattering configuration to simultaneously collect the forward-scattered light in a single-shot multitrack measurement using a high-numerical-aperture condenser. This concept of increasing collection efficiency in Raman spectroscopy has been explored in previous publications [13,14]. However, these approaches rely on special sample substrates to work with increasing complexity compared to using standard coverslips. Thus, most LTRS setups described in the literature work by exclusively collecting either the backscattered or forward-scattered light [15–17]. Since LTRS samples often are transparent, and the setups in general already have a high-numerical-aperture condenser mounted, extending the capabilities to collect both backscattered and forward-scattered light is straightforward. Using this approach, we demonstrate a more sensitive and flexible experimental setup that allows for both confocal and nonconfocal detection. Additionally, we show how to add polarization sensitivity to the setup to measure how the Raman scattering rotates polarization, which depends

on the symmetry of the molecular vibrations [18]. We anticipate that these results can be useful for future studies of sensitive biological systems.

2. EXPERIMENTAL

To trap particles and acquire their Raman spectra, we use a custom-built LTRS instrument built around a modified inverted microscope (IX71, Olympus) previously described in [19–21]; see Fig. 1. In short, we focus an 808 nm continuous-wave laser (CRL-DL808-120-S-US-0.5, CrystaLaser) using a 60× water immersion objective (UPlanSApo60xWIR 1.2NA, Olympus) to form the trap and excite the Raman scattering. Further, we use the objective to collect the backscattered Raman light.

For this study, we modify the setup by adding a 60× oil immersion objective (UPLANAPO60X 1.4NA, Olympus) above the sample to collect the forward-scattered light and act as a condenser to illuminate the sample. We then separate the forward-scattered light and illumination light using a shortpass filter (FESH0750, Thorlabs). After this, we pass the forward-scattered light through a notch filter and an optional confocal pinhole, and then we combine it with the backscattered light using a D-shaped pickoff mirror (PFD10-03-P01, Thorlabs). Next, we depolarize the beams using a depolarizer (DPP25-B, Thorlabs) and direct them to the spectrometer (Model 207, 600lp/mm grating, McPherson), where they are dispersed and imaged on separate tracks on a CCD detector (Newton 920N-BR-DD XW-RECR, Andor). Optionally, for polarization Raman measurements, we instead combine the beams using a

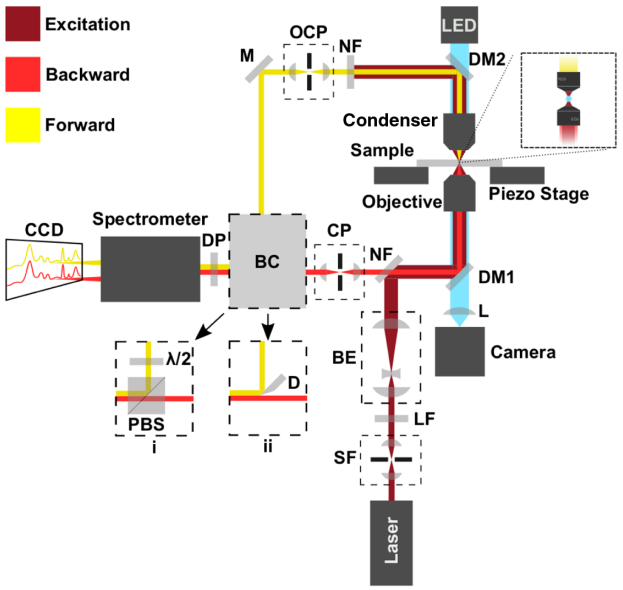

Fig. 1. Illustration of the experimental setup with abbreviated component names. M, mirror; DM1, 750 nm shortpass filter; DM2, 650 nm shortpass filter; PBS, polarizing beam splitter; OCP, optional confocal pinhole; CP, confocal pinhole; SF, spatial filter; BE, beam expansion; L, lens; NF, notch filter; DP, depolarizer; and BC, beam combiner, which has two options. (i) The two beams are merged using a PBS. A half-wave plate rotates the polarization of one beam to select between depolarized and polarized Raman scattering. (ii) A pickoff mirror D is used to combine the beams. The inset shows a zoomed-in view of the sample.

polarizing beam splitter (PBS252, Thorlabs) with a half-wave plate inserted in the forward-scattered beam path. This change allows us to rotate the forward-scattered beam's polarization and select if we want to measure the polarized or depolarized Raman bands. With this setup, we can separately measure the forward- and backscattered light or the polarized and depolarized Raman spectrum in a single shot similar to [18].

To prepare a sample for use in the LTRS setup, we first construct a sample chamber. We prepared a typical sample chamber by adding two pieces of double-sided scotch tape (3M Company) spaced 5 mm apart on a 24.0 × 60.0 mm coverslip (no. 1, Paul Marienfeld GmbH & Co). Then we position a 20.0 × 20.0 mm coverslip (no. 1, Paul Marienfeld GmbH & Co) on top of the tape to form a 5.0 × 20.0 × 0.1 mm^3 chamber. Next, we fill the chamber with our sample liquid of choice by adding a few microliters of liquid at one of the openings and allowing capillary forces to fill the chamber. For this study, this was either 3.1 μm CML polystyrene latex beads (Thermo Fisher Scientific) suspended in either absolute ethanol (VWR International) or Milli-Q (MQ) water, alternatively pure cyclohexane (Honeywell International), or *Bacillus thuringiensis* (*B. thuringiensis*) spores (ATCC 35646) suspended in MQ water. To ensure that all measurements are done on single particles, we dilute the suspensions containing beads or spores so that there is less than one particle per field of view (∼100 × 100 μm) in the microscope. For the beads, this corresponds to a 1:40,000 dilution of our stock solution. Finally, we seal the open ends of the chamber using vacuum grease (Dow Corning).

To measure the Raman spectrum, we mount the sample to the LTRS setup and position the focal plane of the trapping objective ∼30 μm from the top coverslip. Then, we focus the condenser objective to be parfocal with the trapping objective, that is, to have overlapping focal planes. From this position, we can either measure using this parfocal setup or defocus the two objectives by moving the trapping objective up or down. After focusing, we can open the shutter to the laser and trap a particle or illuminate the sample liquid. Additionally, we can choose if we want to use the optional confocal pinhole in the forward scattered beam path for confocal or nonconfocal measurements. Next, we record the Raman spectrum using two accumulations with 5 s exposure time with a laser power of 20 mW. When measuring on spores, we instead use quartz coverslips (25 × 25 mm, 0.2 mm thick, Alfa Aesar) to construct the sample chamber, and we use two accumulations of 30 s and a laser power of 2.5 mW. Before analysis, we background subtract each spectra using asymmetric least squares to get a reliable measure of peak intensity [22]. Thus, all peak intensities are estimated from baseline corrected spectra, while those displayed in the figures are uncorrected to give a true representation of the magnitude of the background.

3. RESULTS AND DISCUSSION

To display our setup's increased collection efficiency, we trap 3.1 μm polystyrene beads in MQ water and measure their Raman spectra with the condenser and objective parfocal to each other with the optional confocal pinhole left out. Configured like this, and taking the sum of the forward- and

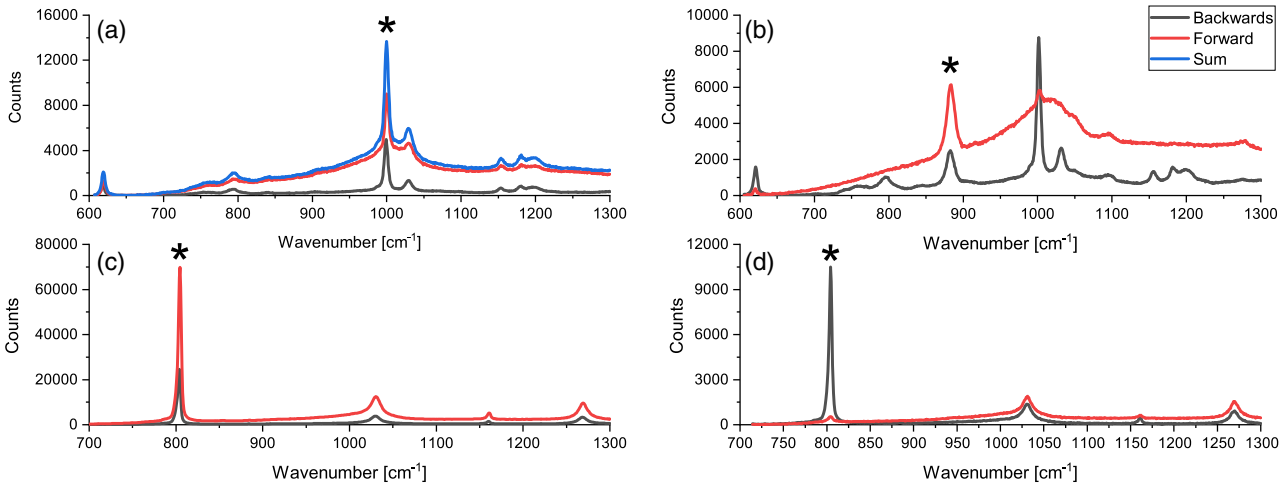

Fig. 2. (A) Backward (black), forward (red), and sum (blue) spectra of a trapped 3.1 μm polystyrene bead in water. Here we measure with the trapping and condenser objective parfocal to each other. (B) A spectrum of a 3.1 μm polystyrene bead trapped in ethanol, which adds a peak at 880 cm^{-1}. Here the trapping and condenser objectives are defocused by 20 μm from each other. (C) Spectrum of cyclohexane using pick-off mirror to combine beams measured with the condenser and trapping objective parfocal to each other. (D) Using a PBS to combine beams and a half-wave plate to rotate the polarization of the forward-scattered beam by 90°. Peaks of interest are marked with asterisks (*).

backward-scattered light, we theoretically collect ∼60% of the total 4π solid angle scattered light from the microparticle and thus more than double the 28% collected solely from the backscattering. This increase in collection efficiency should double the Raman signal if we sum the two detection directions. To verify this experimentally, we compare the intensity of the 1001 cm^{-1} peak between the backscattered spectrum (black) and the sum (blue) and see that the ratio between the two is $2 \pm 0.1 (n = 5)$, close to the expected value of 2 (Fig. 2). The small deviations in the ratio are probably due to minor alignment differences between samples. These results indicate that even though this method adds complexity to alignment, it is still consistent between samples.

As we can see from the acquired spectrum, the forward-scattered light contains a broad background centered on 1000 cm^{-1}, originating from the coverslips that make up the sample chamber and the immersion oil [Fig. 2(A)]. This background is mostly absent from the backscattered signal due to the confocal pinhole filtering it out. A confocal pinhole gives the backscattered light a high spatial specificity, meaning it collects light from a small sample volume. Conversely, the forward-scattered light gathers light from a greater sample volume, lacking a confocal pinhole. This ability to collect light from a larger volume results in the forward-scattered light containing more signal from the sample bulk and thus has more background. As a result, our setup effectively gathers light from both the sample bulk and the trapped object simultaneously, adding experimental flexibility to the setup. For example, this could be useful for studies where the trapped object is put in a chemically changing environment where both the spectrum of the trapped object and its environment are of interest.

To demonstrate this difference in spatial sensitivity between the two detection paths, we measure on 3.1 μm beads suspended in ethanol with the condenser and trapping objective defocused by 20 μm with the optional confocal pinhole left out [Fig. 2(B)]. In this case, we see that the backscattered signal looks the same as before except for an added peak at ∼880 cm^{-1} corresponding to ethanol. However, the forward-scattered signal has altered. The forward-scattered spectrum now shows a faint polystyrene peak at 1001 cm^{-1} and a prominent ethanol peak. If we compare the ethanol peak ratio between the forward-scattered (red) and backscattered (black) spectrum, we get a ratio of ∼2, which implies that we collect twice as much signal in the forward direction. Thus, even when the condenser objective is defocused, it is still twice as efficient as the trapping objective at gathering light from the liquid medium due to its nonconfocal detection. Also, due to the short depth of focus of the condenser objective, ∼0.6 μm, little scattered light from the trapped particle gets gathered. Combining these effects, we can see that this setup allows simultaneous measurement of both the bulk sample and the trapped object.

To investigate our setup's capabilities to measure liquid samples, we filled a sample chamber with cyclohexane and measured with trapping and condenser objective parfocal to each other with the optional confocal pinhole left out [Fig. 2(C)]. In this case, we see that both objectives gather a clear cyclohexane spectrum with characteristic peaks at around 800 cm^{-1}, 1030 cm^{-1}, 1160 cm^{-1}, and 1270 cm^{-1}. However, if we compare the ratio of the ∼800 cm^{-1} peak intensity between the two paths, we see that the forward scattering is ∼2.8 times more efficient. Comparing this to the previous defocused case where we measured on ethanol, we now collect ∼40% more signal. The cause of this increase is likely twofold. First, defocusing separates the excitation laser's and condenser's focal points, lowering the collection efficiency. Second, in the previous case, a particle was trapped, taking up most of the laser's focal volume, hindering it from exciting the liquid. This result indicates that the setup is beneficial when measuring a purely liquid sample where Raman scattering often is weak.

To further display the setup's flexibility, we show how one can add polarization sensitivity to it. We do this by switching out the D-shaped pickoff mirror in the beam combiner with a

PBS. In this configuration, the PBS acts as a beam combiner and analyzer to selectively combine the polarized and depolarized Raman bands. As a demonstration, we add a half-wave plate to the forward-scattered beam path and use it to rotate the polarization by 90° and measure the Raman spectrum of cyclohexane, a chemical with a know polarization dependence [23]. From this measurement, we can see a polarization dependence on the ∼800 cm^{-1} peak and the small peak at ∼1030 cm^{-1}, as they have strongly reduced intensities in the forward-scattered spectrum [Fig. 2(D)]. In contrast to this, the peaks at ∼1160 and ∼1270 cm^{-1} exhibit little polarization dependence with unaffected intensities. As we use an ordinary nonachromatic wave plate and do not know the two beam paths' collection efficiency, we do not get the polarization dependence in absolute values. However, as proof of concept and to measure relative changes in the polarization dependence of the Raman spectrum of a sample, this method provides a fast and straightforward single-shot way of measuring polarized Raman.

To demonstrate the setup using a biological sample, we trapped a *B. thuringiensis* spore and measured its Raman spectrum; see Fig. 3. The data shows a clear *B. thuringiensis* spectrum with characteristic peaks at 650, 820, and 1016 cm^{-1}, related to the calcium-dipicolinic acid (CaDPA) content of the spore core, even with a modest excitation power of 2.5 mW and integration time of two accumulations of 30 s. If we compare the ratio between the 1016 cm^{-1} peaks in the backward-scattered light and the sum of the forward- and backward-scattered light, we get a ratio of ∼2. It is worth noting that we switched out the standard microscope slides with quartz slides and added the optional confocal pinhole to the forward-scattered light to reduce the background noise. The remaining broad background centered on 1000 cm^{-1} in the signal probably originates from the immersion oil used to collect the forward-scattered light and could be removed by migrating to a water immersion objective. Thus, we can conclude that this method doubles the signal intensity, even with a confocal pinhole in the forward-scattered light path. As photodamage is an effect that depends linearly on laser power, this means that a doubled collection efficiency allows for a halved photodamage rate, which in turn allows for twice as long measurements without extra photodamage. Additionally, to demonstrate that the trapping stays stable even at low powers, we trapped both *B. thuringiensis* spores and vegetative cells with a power of 0.5 mW. Doing this, we observed that both particle types remained stably trapped for more than 10 min.

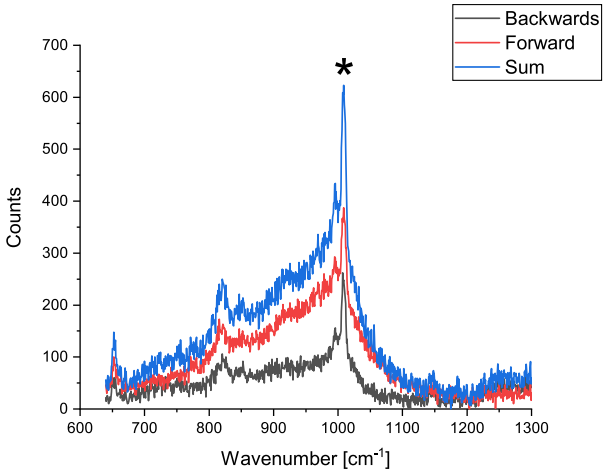

Fig. 3. Spectrum of a single trapped *B. thuringiensis* spore measured using only backward scattering (black), only forward scattering (red), and a sum of forward and backward scattering (blue). The main peak related to the CaDPA content of the spore is marked with an asterisk (*).

4. CONCLUSIONS

We demonstrate a simple-to-implement method that provides a more sensitive and flexible LTRS setup. The added sensitivity allows for decreased laser power and thus reduced photodamage to the sample as well as faster acquisition times. Further, the setup gives the flexibility to measure with the pinpoint spatial selectivity of confocal Raman spectroscopy and the bulk sensitivity of nonconfocal Raman spectroscopy simultaneously. Lastly, the setup can measure relative changes in a sample's polarized Raman spectrum in a single shot. We envision the setup being used for faster, less invasive, and more flexible chemical fingerprinting of biological particles.

Funding. Stiftelsen för Strategisk Forskning; Vetenskapsrådet (2019-04016).

Disclosures. The authors declare no conflicts of interest.

Data Availability. Data underlying the results presented in this paper are not publicly available at this time but may be obtained from the authors upon reasonable request.

REFERENCES

1. R. Thurn and W. Kiefer, "Raman-microsampling technique applying optical levitation by radiation pressure," Appl. Spectrosc. **38**, 78–83 (1984).
2. B. Redding, M. Schwab, and Y.-L. Pan, "Raman spectroscopy of optically trapped single biological micro-particles," Sensors **15**, 19021–19046 (2015).
3. D. Chen, S. S. Huang, and Y. Q. Li, "Real-time detection of kinetic germination and heterogeneity of single *Bacillus* spores by laser tweezers Raman spectroscopy," Anal. Chem. **78**, 6936–6941 (2006).
4. P. Zhang, L. Kong, P. Setlow, and Y.-Q. Li, "Characterization of wet-heat inactivation of single spores of *bacillus* species by dual-trap Raman spectroscopy and elastic light scattering," Appl. Environ. Microbiol. **76**, 1796–1805 (2010).
5. S. Rao, Š. Bálint, B. Cossins, V. Guallar, and D. Petrov, "Raman study of mechanically induced oxygenation state transition of red blood cells using optical tweezers," Biophys. J. **96**, 209–216 (2009).
6. A. Bankapur, S. Barkur, S. Chidangil, and D. Mathur, "A micro-Raman study of live, single red blood cells (RBCS) treated with agno3 nanoparticles," PLOS One **9**, e103493 (2014).
7. N. Kuhar, S. Sil, T. Verma, and S. Umapathy, "Challenges in application of Raman spectroscopy to biology and materials," RSC Adv. **8**, 25888–25908 (2018).
8. Z. Pilát, S. Bernatová, J. Ježek, J. Kirchhoff, A. Tannert, U. Neugebauer, O. Samek, and P. Zemánek, "Microfluidic cultivation and laser tweezers Raman spectroscopy of *E. coli* under antibiotic stress," Sensors **18**, 1623 (2018).
9. S. S. Huang, D. Chen, P. L. Pelczar, V. R. Vepachedu, P. Setlow, and Y. Q. Li, "Levels of Ca^{2+}-dipicolinic acid in individual *Bacillus* spores determined using microfluidic Raman tweezers," J. Bacteriol. **189**, 4681–4687 (2007).
10. A. Blázquez-Castro, "Optical tweezers: phototoxicity and thermal stress in cells and biomolecules," Micromachines **10**, 507 (2019).
11. R. R. Jones, D. C. Hooper, L. Zhang, D. Wolverson, and V. K. Valev, "Raman techniques: fundamentals and frontiers," Nanoscale Res. Lett. **14**, 231 (2019).

12. C. Zong, M. Xu, L. J. Xu, T. Wei, X. Ma, X. S. Zheng, R. Hu, and B. Ren, "Surface-enhanced Raman spectroscopy for bioanalysis: reliability and challenges," Chem. Rev. **118**, 4946–4980 (2018).
13. A. K. Misra, S. K. Sharma, L. Kamemoto, P. V. Zinin, Q. Yu, N. Hu, and L. Melnick, "Novel micro-cavity substrates for improving the Raman signal from submicrometer size materials," Appl. Spectrosc. **63**, 373–377 (2009).
14. M. Y. Wu, D. X. Ling, L. Ling, W. Li, and Y. Q. Li, "Stable optical trapping and sensitive characterization of nanostructures using standing-wave Raman tweezers," Sci. Rep. **7**, 1–8 (2017).
15. T. J. Harvey, E. C. Faria, A. Henderson, E. Gazi, A. D. Ward, N. W. Clarke, M. D. Brown, R. D. Snook, and P. Gardner, "Spectral discrimination of live prostate and bladder cancer cell lines using Raman optical tweezers," J. Biomed. Opt. **13**, 064004 (2008).
16. J. Lin, L. Shao, S. Qiu, X. Huang, M. Liu, Z. Zheng, D. Lin, Y. Xu, Z. Li, Y. Lin, R. Chen, and S. Feng, "Application of a near-infrared laser tweezers Raman spectroscopy system for label-free analysis and differentiation of diabetic red blood cells," Biomed. Opt. Express **9**, 984–993 (2018).
17. J. Lukose, N. Mithun, G. Mohan, S. Shastry, and S. Chidangil, "Normal saline-induced deoxygenation of red blood cells probed by optical tweezers combined with the micro-Raman technique," RSC Adv. **9**, 7878–7884 (2019).
18. P. Zhang, P. Setlow, and Y. Li, "Characterization of single heat-activated *bacillus* spores using laser tweezers Raman spectroscopy," Opt. Express **17**, 16480–16491 (2009).
19. T. Stangner, T. Dahlberg, P. Svenmarker, J. Zakrisson, K. Wiklund, L. B. Oddershede, and M. Andersson, "Cooke–triplet tweezers: more compact, robust, and efficient optical tweezers," Opt. Lett. **43**, 1990–1993 (2018).
20. T. Dahlberg, D. Malyshev, P. O. Andersson, and M. Andersson, "Biophysical fingerprinting of single bacterial spores using laser Raman optical tweezers," Proc. SPIE **11416J**, 156–162 (2020).
21. D. Malyshev, T. Dahlberg, K. Wiklund, P. O. Andersson, S. Henriksson, and M. Andersson, "Mode of action of disinfection chemicals on the bacterial spore structure and their Raman spectra," Anal. Chem. **93**, 3146–3153 (2021).
22. S. He, W. Zhang, L. Liu, Y. Huang, J. He, W. Xie, P. Wu, and C. Du, "Baseline correction for Raman spectra using an improved asymmetric least squares method," Anal. Methods **6**, 4402–4407 (2014).
23. E. Ly, O. Piot, A. Durlach, P. Bernard, and M. Manfait, "Polarized Raman microspectroscopy can reveal structural changes of peritumoral dermis in basal cell carcinoma," Appl. Spectrosc. **62**, 1088–1094 (2008).